PROBABILISTIC FORECASTS OF WELL FLOW RATE AND SPACING FOR LOW ENTHALPY GEOTHERMAL PROJECTS

Thomas Schaaf[1], Patrick Egermann[1], Delphine Patriarche[1] and Marie-Paule Promis[1]

[1] STORENGY, ENGIE Group, 12 rue Raoul Nordling 92274 Bois-Colombes cedex, France

thomas.schaaf@storengy.com

Keywords: Uncertainty quantification, probabilistic forecasts, well spacing, Dogger formation, Basin of Paris.

ABSTRACT

Like in the oil and gas business or mining industry, getting reliable production forecasts is a key aspect of any geothermal project. Our application cases are low enthalpy projects, located in the Paris Basin and exploiting the Dogger formation. Typical development plan consists of a doublet (a pair of one injector and one producer wells) which long-term sustainable flow rates and thermal breakthrough timing should be thoroughly assessed.

Properly analyzing and quantifying the technical and economical uncertainties allows for deciding the development of such a project. Focusing on the subsurface uncertainties, we have to quantify the ones that may impact a geothermal well productivity/injectivity. Such uncertain static parameters could include for example the net pay, the permeability, the well skin or the expected pressure and temperature at reservoir level.

Using the power of geostatistics, which allow estimating and simulating the spatial variability of the properties we are interested in, together with advanced workflow capabilities of geomodelling software, we are then able to generate hundreds of equiprobable realizations for each of the properties considered and to extract key statistics for a prospect zone. These realizations are conditioned to the data gathered on existing wells in the nearby zone. Those distributions, in a probabilistic view, quantify the uncertainty on the subsurface and can be inputs for the dynamic modelling part.

This dynamic modelling , for a fixed well architecture and a given surface facilities operating pressure, computes the pressure drops in the reservoir and the well. Using the nodal analysis, for the given reservoir and well properties, we estimate what might be the flow rate and associated flowing reservoir pressure. Accordingly, we estimate the extra pressure drop that is needed to achieve a target rate as well as simulate the use of a down-hole pump.

Finally, for each of the target rates, a distribution of drawdowns (associated to the subsurface uncertainties) is obtained. We are then able, for a given maximum drawdown value (derived from the well architecture) to derive the probability of achieving target flow rates. This approach has also been coupled with an analytical formula to estimate the associated optimal well spacing value for several values of nominal rate and thermal breakthrough time.

Using this workflow has made possible to get probabilistic forecasts of flow rate and well spacing and give properly the uncertainty assessment of any low enthalpy geothermal project capacity and performance, which are of primary importance for decision making.

1. INTRODUCTION

1.1 Context

The challenge we are facing here is the development of low enthalpy geothermal projects, used most of the time for districts heating purpose, in the Parisian Basin. The Dogger formation (Middle Jurassic) is by far the main geothermal reservoir in the Basin (few alternatives are exploiting the Albian formation – Early Cretaceous). A typical development in the Dogger relies in a doublet i.e. one production and one re-injection wells. Since the seventies, tens of doublets have been or are producing, mostly in the North and South-East of Paris (Fig. 1). The Dogger geological interval (fractured oolithic limestone) is then known quite extensively in the area, from geothermal but also from oil and gas exploration activities in a wider area. The Dogger exhibits most of the time good productivity (through few major producing intervals). Nevertheless, some rapid lateral variations may be encountered at the producer-injector distance scale.

Conducting a proper reservoir characterization (possibly through numerical reservoir modelling) would then be useful to assess properly the productivity of a future doublet and the associated uncertainties in terms of flow rates and required well spacing.

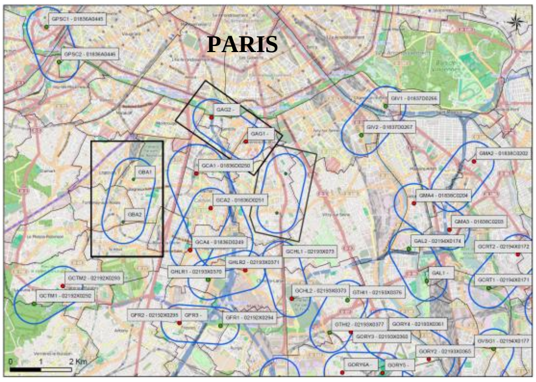

Figure 1: Zoom on past and existing Dogger geothermal doublets located to the South-East of Paris City.

1.2 Motivations

Before developing any project, a proper risk analysis and uncertainty quantification should be performed. These should embrace both technical (subsurface and surface facilities) and economical parameters/inputs, all impacting the key properties/outputs which would be looked at to make an investment decision : validate or not the project. This approach is common to many subsurface resources based projects (oil & gas, mining, etc.). It could be summarized, in a simplified way, by a list of uncertain input parameters which, through some modelling steps (analytical and/or numerical) would generate some results/outputs of interest. Those outputs are finally analysed to make a decision (Fig. 2).

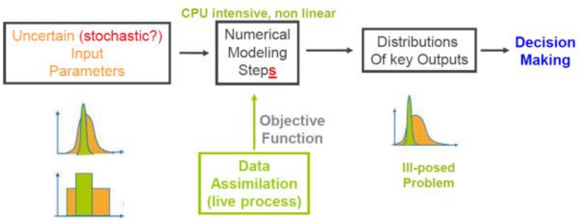

Figure 2: Uncertainty quantification and risk analysis workflow for decision making

Depending on the project phase (exploration, development, production), more or less data/observations are available. The (numerical) models used should be history matched to those data (i.e. moving from the *a priori* - green - to the *a posteriori* - orange – distributions; Fig. 2). Mathematically speaking, this is a non-linear inverse problem, quite common in (Earth Sciences) engineering (Caers 2011, Magnusdottir and Horne 2015). It is a necessary but not sufficient step to get reliable production forecasts (Schaaf et al. 2009a).

This paper is focusing on the subsurface uncertainties (e.g. net pay zone, porosity), looking at well flow rates sustainability (typically over 30 years) and minimum well spacing required to avoid any thermal breakthrough over the same period (Gringarten and Sauty 1975, Satman 2011, Ganguly and Kumar 2014). Assessing properly the uncertainty associated to the producer well temperature and flow rate evolution over time is a key aspect of any geothermal doublet project (Ungemach et al. 2011).

It should be pointed out that the approach we are proposing is quite modular and versatile. It could be applied and extended actually to any type of geothermal projects (i.e. High Enthalpy as well) or modelling tools as long as the associated module/block is updated accordingly.

2. SUBSURFACE STATIC PROPERTIES UNCERTAINTY QUANTIFICATION

The above described approach is applied for a study aiming at assessing the geothermal potential over an area which has not been extensively developed to date. We are clearly in the context of exploration or pre-development phases with few data (mostly static ones from nearby wells). The detailed wells architecture and completion are not yet designed at this stage so a Dogger generic well architecture (Fig. 3) is assumed:

- slanted well with a deviation of about 40°,

- 9’’5/8 tubing,

- open-hole at the reservoir face.

The flow rate of a well depends on the pressure drop generated between the far field reservoir and the well head (including the positive effect of a down-hole pump). This pressure drop may be split in two components (Fig. 3):

(a) a pressure drop ΔP1 which is the difference between the reservoir pressure Pres and the bottom-hole well flowing pressure (reservoir face) Pwf. This pressure drop times the well productivity index gives the down hole flow rate,

(b) a pressure drop ΔP2 which is the difference between the well flowing pressure Pwf and the tubing head pressure THP. This pressure drop is a result of the gravity, friction and acceleration effects. Only the gravity effect would be considered here. A down hole pump would impact this ΔP2 value by increasing the pressure value at a certain depth near the surface.

Regarding the point (a), subsurface uncertainties would come from:

- the reservoir net pay (parameter n°1), the permeability (or transmissibility, parameter n°2) and the skin (parameter n°3) which would all modify the well productivity index,

- the Dogger top reservoir depth (parameter n°4) combined with the pressure and temperature gradients (parameters n°5 & 6) would modify the reservoir pressure and temperature (and therefore the viscosity and density of the water).

Regarding the point (b), for a set well architecture, the Dogger top reservoir depth would modify the length of the 9’’5/8 tubing above the open hole section.

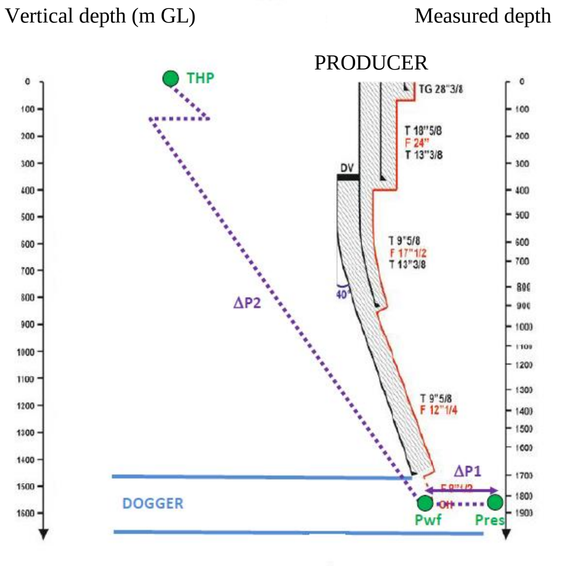

Figure 3: Generic Dogger (producer) well architecture and associated pressure drops

We have identified six parameters which would impact pressure drop(s) and thus the resulting well flow rate. A proper uncertainty quantification should then be performed on those parameters to derive the associated uncertainty on the flow rate for a given location in the area of interest.

2.1 Key subsurface properties uncertainty assessment

At the scale of the Parisian Basin, many geothermal wells have been drilled over an area broadly centred on the city of Paris (Fig. 4). They carry useful data/information gathered into a well database (~40 wells; Munoz 2015). Each well is a conditioning point (hard data) of key subsurface properties as for instance the reservoir net pay (Fig. 5). Once again, quite large variations may be observed on the values over short distance ranges (at least of the same order as the producer-injector top reservoir spacing). Other key properties gathered in the database concern the permeability/transmissibility, the porosity, the salinity, the reservoir pressure and temperature as well as the artesian flow rates if any.

To assess the spatial variability of those static properties (which would impact the wells productivity and their spacing), we are using a tool dedicated to this purpose: the geostatistics (Chambers et al. 2000a&b, Yarus and Chambers 2006, Daily and Caers 2010). Geostatistics allow to estimate and simulate the spatial variability (in 2D or 3D) of any property we are interested in. By defining typical inputs such as a histogram, correlation length and a variogram, the user might generate as many equiprobable geostatistical realizations as requested. This is done by changing the seed number, an integer value which determines the random path over the discretized grid. Using N different seeds will generate N alternative, equiprobable realizations having the same mean, variance, etc. Hard data conditioning is achieved through a kriging step. Feedbacks on the use of geostatistics show that the most difficult part is to infer the horizontal correlation lengths to get relevant properties between the wells. A large uncertainty is therefore associated to them which makes even more important the type of analysis conducted in this study.

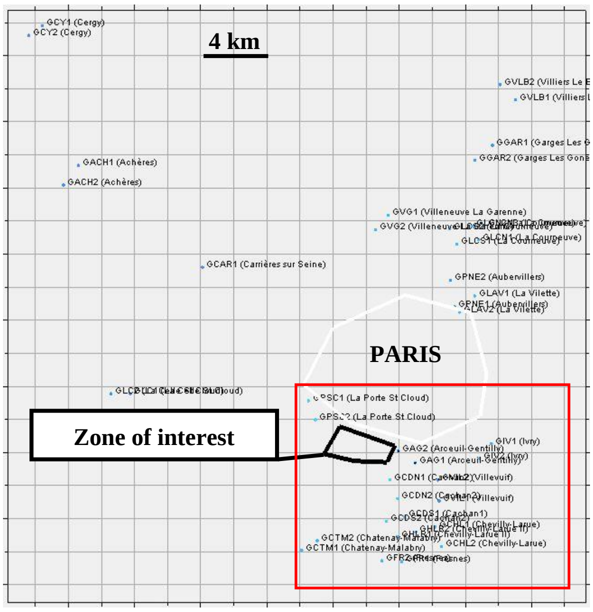

Figure 4: Geothermal wells location considered for the geostatistical studies

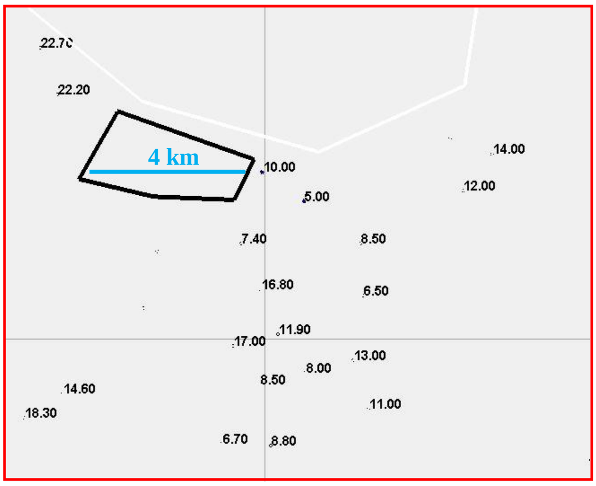

Figure 5: Example of wells location used as conditioning points for the reservoir net pay

Using the well database, it is assumed here that inferred statistics from a pool of 40+ samples (i.e. wells) lead to relevant figures. The mean, variance and histogram of all static properties (e.g. net pay; Fig. 6) can then be computed. The two degrees of freedom which are left are the correlation lengths and the seed number.

Using a geomodelling software and a standard geostatistical algorithm (Sequential Gaussian Simulation, Deutsch and Journel 1997), a geostatistical realization (conditioned to hard well data) can be simulated. Fig. 7 is an example of realization among many others for the reservoir net pay property.

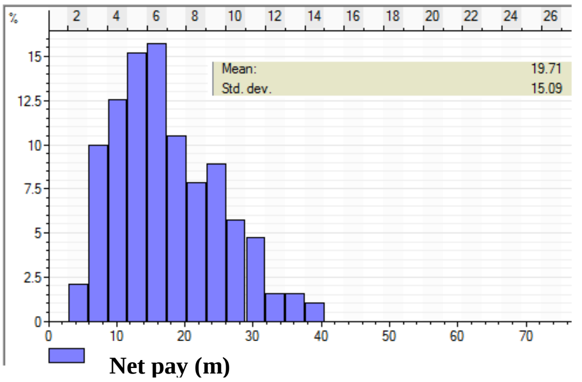

Figure 6: Histogram and statistics for the reservoir net pay from the 40+ wells

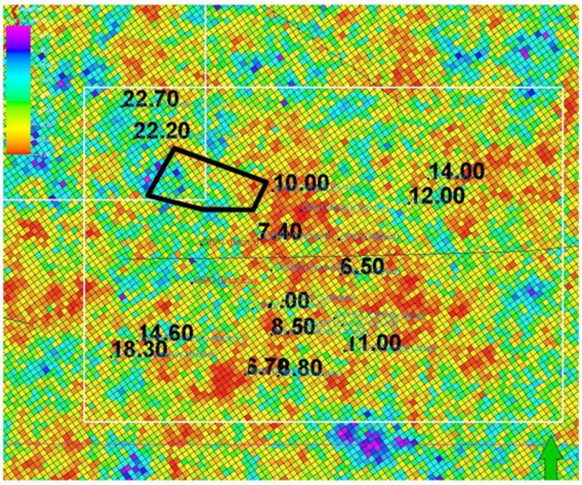

Figure 7: Example of geostatistical realization for the net pay (together with the conditioning points)

Such realization might be filtered out over the polygon of interest only (i.e. the surface area where the well pad and surface facilities could be implemented). Minimum, Maximum, mean and variance values are then derived. Using all the workflow manager functionalities of a geomodelling software (SCHLUMBERGER 2014, Schaaf et al. 2009b), we are able to automate this process and to generate a Monte Carlo sampling (200 samples) over the two main uncertain parameters:

- the seed number, interval [1,32000],
- and the correlation length , interval [750,1500]m.

Results are written down and exported by the workflow. From sample to sample, quite large variations may be encountered (Fig. 8). Such variations would depend mostly over the distance of conditioning points with respect to the polygon together with the correlation lengths considered.

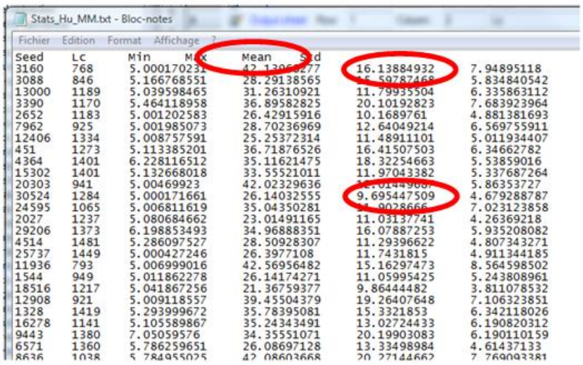
Stats_Hu_MM.txt - Bloc-notes

Fichier Edition Format Affichage ?

Seed	Lc	Min	Max	Mean	Std
3160	768	5.000170231	[illegible]	16.13884932	7.94895118
3088	846	5.166768551	28.29138565	[illegible]	5.834840542
13000	1189	5.039598465	31.26310921	11.79935504	6.335863112
3390	1170	5.464118958	36.89582825	20.10192823	7.683923964
2652	1183	5.001202583	26.42915916	10.1689761	4.881381693
7962	925	5.001985073	28.70236969	12.64049214	6.569755911
12406	1334	5.008757591	25.25372314	11.48911101	5.011934407
451	1273	5.113385201	36.71876526	16.41507503	6.34662782
4364	1401	6.228116512	35.11621475	18.32254663	5.53859016
15302	1401	5.132668018	33.55521011	11.97043382	5.337687264
20303	941	5.00469923	42.02329636	[illegible]	5.86353727
30524	1284	5.000171661	26.14032555	9.695447509	4.679288787
24595	1065	5.006811619	35.04350281	[illegible]	7.023123858
2027	1237	5.080684662	23.01491165	11.03137741	4.26369218
29206	1373	6.198853493	34.96888351	16.07887253	5.935208082
4514	1481	5.286097527	28.50928307	11.29396622	4.807343271
25737	1449	5.000427246	26.3977108	11.7431815	4.911344185
11936	793	5.006999016	42.56956482	15.16297473	8.564598502
1544	949	5.011862278	26.14174271	11.05995425	5.243808961
18516	1217	5.041867256	21.36759377	9.86444482	3.811078532
12908	921	5.009118557	39.45504379	19.26407648	7.106323851
1328	1419	5.293999672	35.78395081	15.3321853	6.342118026
16278	1141	5.105589867	35.24343491	13.02724433	6.190820312
9443	1380	7.05059576	34.35551071	20.19903083	6.190110159
6571	1360	5.786259651	26.08697128	13.33498984	4.61437133
8636	1038	5.784955025	42.08603668	20.27144662	7.769093381

Figure 8: Extract of the results file for the net pay

2.2 Real field case application case: Statistics for a prospect zone next to Paris

Repeating this workflow for each of the key property, the analysis of the 200 samples leads to the statistics and associated uncertainty over the zone of interest (Table 1). Permeability has been co-simulated (with the porosity as secondary variable). Pressure and temperature realizations have been co-simulated (with a trend map based on the top Dogger horizon depth).

Table 1: Statistics for the net pay and others key properties over the zone of interest

	Minimum	Maximum	Mean	Variance
Net pay (m)	5	47.4	15.1	6.3
Porosity (%)	5	25.2	14.9	2.25
Permeability (D)	0.1	7	1.7	1.15
Reservoir pressure (bar)	150.5	162	156.6	1.2
Reservoir temperature (°C)	57	66	61.9	0.9

3. PROBABILISTIC FLOW RATE FORECASTS

3.1 Dynamic modelling of the reservoir-well system

The dynamics of the reservoir/well couple is made through a nodal analysis (routine use in the oil & gas industry, Fig. 9) which enables the rapid calculation of the operating point from the crossing point of two curves:

- the inflow performance curve (orange curve, Fig. 9), which is derived from the reservoir static properties and pressure. It gives access to the evolution of the pressure drop ΔP1 as a function of the flowrate (point (a), paragraph 2),

- the vertical lift performance curve (pink curve, Fig. 9), which is derived from the well and completion architectures, the flowing fluids properties and the expected tubing head pressure. It gives access to the evolution of the pressure drop ΔP2 as a function of the flowrate (point (b), paragraph 2), For the inflow performance curve, changing the sole net pay value would change the slope but not its Y-axis intercept. Accordingly, changing the sole reservoir pressure would modify the Y-axis intercept while keeping the same slope.

For the vertical lift performance curve, changing the tubing size would change the shape but not its Y-axis intercept. Accordingly, changing the reference tubing head pressure would change the Y-axis intercept but not the shape itself. For the required tubing head pressure value, the Y and X coordinates of the operating point give access to respectively the well flowing pressure and the well flowing rate.

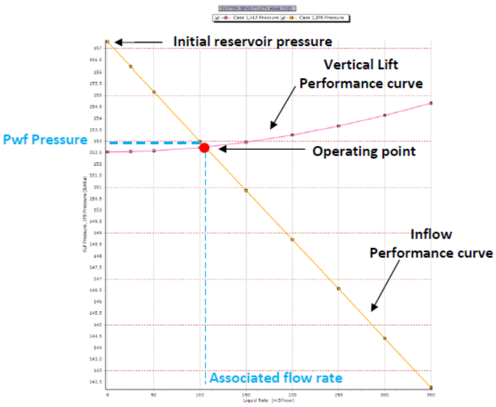

Figure 9: Example of nodal analysis

As the tubing head pressure is assumed defined at 5 bar and the well architecture is set, the Vertical Lift Performance curve would almost not change. Very minor variations might come from the slight change in the 9''5/8 tubing length (uncertainty on the Dogger top horizon depth).

3.2 Modelling the impact of a down-hole pump

Following the same logic, the extra pressure support (X bar) of a down hole pump could be mimicked by a vertical shift of X bar of the inflow performance curve. In other words, a pump giving X bar of pressure support is modelled as a reservoir having its initial pressure boosted by X bar.

Conducting a nodal analysis for a full set of pressure support values gives access to the extra pressure boost needed to achieve a target flow rate.

Fig. 10 shows an example where the reservoir properties would lead to a geothermal well having an artesian flow rate of 100 m^3/h with a tubing head pressure of 5 bar. Producing this well at a 250 m^3/h would require an extra pressure support of ~7 bar. This pressure support value can be directly translated into a variation of the liquid level in the annular space (called drawdown later in the paper) for an optimal positioning of the downhole pump.

The same analysis can be conducted for different target well flow rates. Well flow rates values of 200, 250 and 350 m^3/h are considered. Also, such nodal analysis could be used to double check well test results.

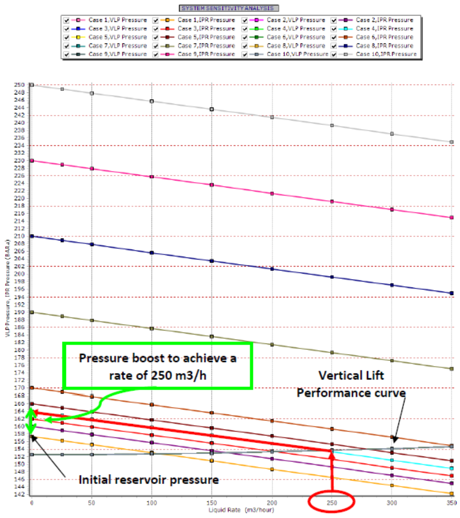

Figure 10: Modelling the impact of a down hole pump

3.3 Risk analysis: uncertainty distributions of targeted flow rates

Given the statistics of key properties (Table 1) and using a sampling algorithm (Latin Hyper cube design) from a dedicated software (BEICIP FRANLAB 2015), 50 samples are generated. Those 50 samples correspond to 50 alternative reservoir/well couples.

Drawdown values obtained from the nodal analysis are increased of 10 bar (around 100 m) to avoid any risk of pump cavitation (from the well database, the saturation pressure mean value is about 5.5 bar). Appendix A summarizes the results for those 50 samples.

From this probabilistic approach based on 50 samples, the results are analysed in terms of histograms and cumulative probabilities. Fig. 11 indicates the frequency of drawdown ranges for a target flow rate of 200 m^3/h for a tubing head pressure of 5 bar, given the subsurface uncertainties which were identified and quantified.

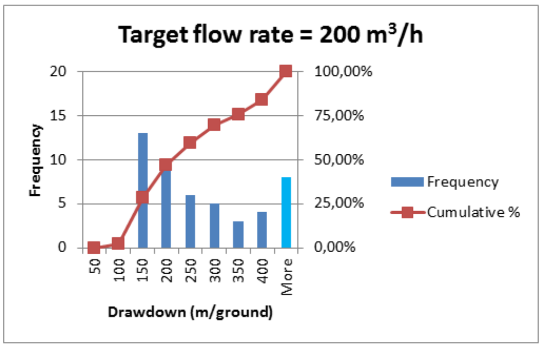

Figure 11: Draw-down frequencies for a target flow rate of 200 m^3/h

Table 2 summarizes all the results obtained for the zone of interest. For instance, if we assume 300 m as the maximum drawdown value, there are 70, 54 and 46 % probabilities to achieve respectively 200, 250 and 350 m^3/h. For each flow rates, the drawn-down ranges which are the closest to the P50 (cumulative probability of 50 %, most likely case) are highlighted in green.

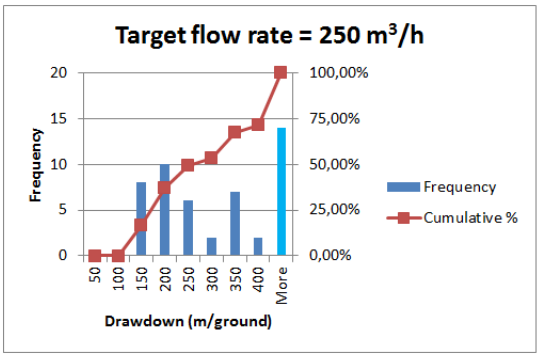

Figure 12: Draw-down frequencies for a target flow rate of 250 m^3/h

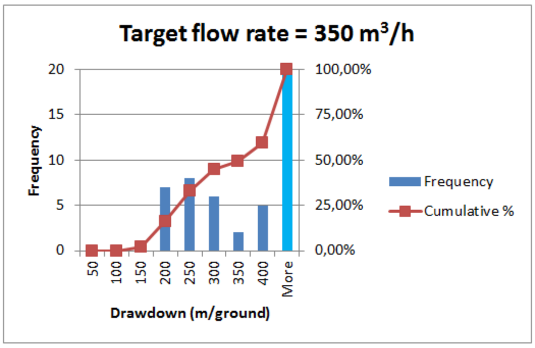

Figure 13: Draw-down frequencies for a maximum flow rate of 250 m^3/h

Table 2: Probabilities of draw-down ranges as a function of target flow rates

Draw-down range (m)	Probability (%) @ flow rate = 200 m^3/h		Probability (%) @ flow rate = 250 m^3/h		Probability (%) @ flow rate = 350 m^3/h	
	Gross	cumulative	Gross	cumulative	Gross	cumulative
50-100	2	2	0	0	0	0
100-150	28	30	18	18	4	4
150-200	18	48	20	38	14	18
200-250	12	60	12	50	16	34
250-300	10	70	4	54	12	46
300-350	6	76	14	68	4	50
350-400	8	84	4	72	10	60
400+	16	100	28	100	40	100

4. PROBABILISTIC WELL SPACING FORECASTS

4.1 Analytical well spacing approach

For a set reservoir model, Gringarten and Sauty (1975) have derived an analytical formula computing the spacing between the wells at which thermal breakthrough would occur for a given flow rate and a given period. Appendix B details the full list of parameters used as well as the default values considered.

This formula is derived for a geothermal reservoir bounded by a top and bottom aquitards. It does not take into account any intermediate ones, which would exchange more heat with the flowing water and thus delay the thermal breakthrough. This analytical formula could then be considered as conservative which is well suited for the uncertainty quantification conducted.

On top of the two target well flow rates of 200 and 250 m^3/h, three exploitation periods are considered : 20, 25 and 30 years.

4.2 Risk analysis: uncertainty distributions of well spacing for targeted flow rates

Fig. 14 represents the spacing distributions at 20, 25 and 30 years for a target flow rate of 200 m^3/h. Most likely spacing values are of 1400, 1850 and 2000 m for respectively 20, 25 and 30 years. For information, considering a kick-off point at 420 m (generic well architecture) and a top Dogger horizon depth of ~1500 m/ground would lead to an operational spacing of ~1800 m. This value corresponds to the red dots in Fig. 14.

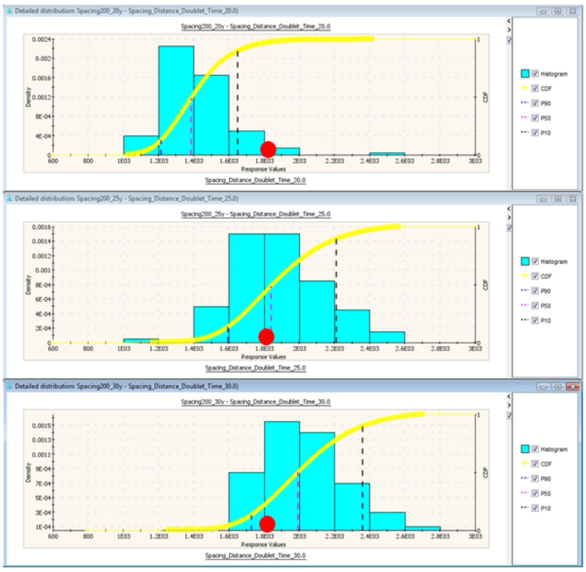

Figure 14: Spacing distributions at 20, 25 and 30 years for a target flow rate of 200 m^3/h

Fig. 15 represents the spacing distributions at 20, 25 and 30 years for a target flow rate of 250 m^3/h. Most likely spacing values are of 1900, 2050 and 2200 m for respectively 20, 25 and 30 years.

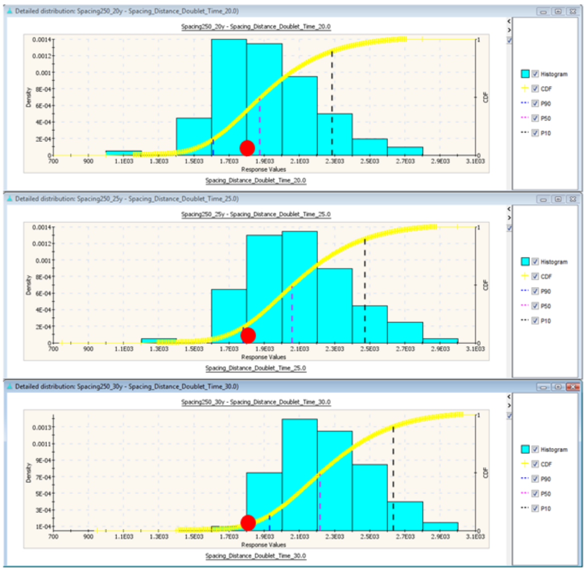

Figure 15: Spacing distributions at 20, 25 and 30 years for a target flow rate of 250 m^3/h

5. CONCLUSIONS AND PERSPECTIVES

We have conducted a proper uncertainty quantification and risk analysis to assess the potential of a geothermal project over a zone of interest in the Parisian Basin.

Analysing and quantifying the uncertainties associated to key subsurface properties have led to probabilistic flow rate and well spacing distributions.

Considering those distributions for decision making and not a few “deterministic” cases (typically P10/P50/P90 values) allows to embrace the full impact of subsurface uncertainties.

The proposed approach is versatile. Surface facilities or even economical uncertain inputs could be for instance considered in the analysis (ESMAP 2012). More detailed 3D numerical simulations could be performed as well (Pruess et al. 1999, Wong et al. 2015). Also the software and workflows used would allow to conduct proper sensitivity analysis and history matching if needed.

REFERENCES

BEICIP FRANLAB: COUGAR© 2015 User’s Guide, *Beicip Franlab*, 2015.

Caers, J.: Modeling Uncertainty in the Earth Sciences, *Wiley-Blackwell*, Oxford, 2011.

Chambers, R.L. et al.: Petroleum Geostatistics for Nongeostatisticians – Part 1, *The Leading Edge*, May 2000, 474-479.

Chambers, R.L. et al.: Petroleum Geostatistics for Nongeostatisticians – Part 2, *The Leading Edge*, June 2000, 592-599.

Daily, C. and Caers, J.: Multi-point Geostatistics – An Introductory Overview, *First Break*, vol. 28, September 2010, 39-47.

Deutsch, C. and Journel, A.: GSLIB: Geostatistical Software Library and User’s Guide, *Oxford University Press*, Oxford, 1997.

ESMAP: Geothermal Handbook : Planning and Financing Power Generation, *The International Bank For Reconstruction And Development*, Washington D.C., 2012.

Ganguly, S. and Mohan Kumar, M.S.: Analytical Solutions for Movements of Cold Water Thermal Front in a Heterogeneous Geothermal Reservoir, *Applied Mathematical Modelling*, n°38, (2014), 451-463.

Gringarten, A. and Sauty, J-P.: A Theoretical Study of Heat Extraction From Aquifers With Uniform Regional Flow, *Journal of Geophysical Research*, vol. 80, n°35, December 1975.

Magnusdottir, L. and Horne, R.N.: Inversion of Time-Lapse Potential Data to Estimate Fracture Connectivity in Geothermal Reservoirs, *Mathematical Geosciences*, n°47, (2015), 85-104.

Munoz, A.: Inventaire des informations techniques sur les puits géothermiques du Lusitanien et du Dogger du Bassin Parisien, Internal report STORENGY, OI-CE/DESS-DPA-2015.00229 (2015).

Pruess, K., Oldenburg, C. and Moridis, G.: TOUGH2 User’s Guide – Version 2.0, *Lawrence Berkeley National Laboratory*, Berkeley, 1999.

Satman, A.: Sustainability, *Proceedings Thirty-Six Workshop on Geothermal Reservoir Engineering Stanford University*, Stanford, California, (2011), SGP-TR-191.

Schaaf, T., Coureaud, B., Labat, N. and Busby, D.: Using Experimental Designs, Assisted History-Matching Tools, and Bayesian Framework To Get Probabilistic Gas-Storage Pressure Forecasts, *SPE Reservoir Evaluation & Engineering Journal*, SPE #113498, October 2009, 724-736.

Schaaf, T., Coureaud, B., and Labaune, F.: Joint Structural and Petrophysical History Matching Leads to Global Geological Stochastic Reservoir Models, *Proceedings of the 2009 SPE Europec/EAGE Annual Conference*, Amsterdam, The Netherlands, (2009), SPE #121899.

SCHLUMBERGER: PETREL© 2014 User’s Guide, *Schlumberger*, 2014.

Ungemach, P., Antics, M. and Lalos, P.: Sustainable Geothermal Reservoir Management, *Proceedings of the Australian Geothermal Energy Conference 2011*, Melbourne, Australia, (2011), 267-275.

Wong, Z.Y., Horne, R. and Voskov, D.: A Geothermal Reservoir Simulator with AD-GPRS, *Proceedings of the World Geothermal Congress 2015*, Melbourne, Australia, (2015), SGP-TR-204.

Yarus, J.M. and Chambers, R.L.: Practical Geostatistics – An Armchair Overview for Petroleum Reservoir Engineers, *Journal of Petroleum Technology*, November 2006, 78-87.

Acknowledgements

We would like to thank our colleagues for fruitful discussions and STORENGY for the permission to publish this work.

APPENDIX A

Drawdown values (including the equivalent 10 bar security margin) lower than 400 m (the kick off point being at 420 m GL in the generic well architecture) are validated. These values are highlighted in green over the three most right columns.

					Q=200m3/h	Q=250m3/h	Qmax=350M3/h
					Net drawdown + 10 b cavitation		
Net Pay (m)	Perm (D)	skin	P (bar)	T (°C)	Net drawdown	Net drawdown	Net drawdown
24,8	2,4	-1,2	158,7	63,0	100,1	113,1	133,1
6,1	1,7	-1,0	156,3	60,6	387,4	457,4	617,4
15,6	0,6	-1,1	158,1	62,5	368,8	448,8	628,8
22,4	0,6	-2,3	156,4	61,7	255,5	305,5	405,5
3,9	1,0	-2,4	157,7	62,1	673,2	843,2	1173,2
2,0	3,3	-1,1	150,0	61,1	600,0	720,0	970,0
16,9	1,1	-1,9	156,6	66,0	203,7	243,7	313,7
19,1	0,8	-1,4	156,8	62,1	252,5	302,5	412,5
19,9	0,8	-1,8	157,0	61,5	229,9	279,9	369,9
19,4	0,1	-1,7	156,5	62,0	1534,9	1465,1	1465,1
14,0	4,0	-1,6	155,8	61,6	122,3	142,3	182,3
8,2	1,5	-0,9	156,9	61,8	310,6	390,6	510,6
15,0	3,6	-2,5	155,2	61,3	118,0	138,0	168,0
9,7	1,6	-4,0	156,3	61,9	176,8	206,8	276,8
23,9	1,8	-1,6	157,4	62,6	126,5	146,5	186,5
16,3	2,2	-1,5	157,4	62,7	135,7	165,7	215,7
11,7	2,8	-0,9	158,3	62,9	147,3	177,3	227,3
17,3	2,1	-1,6	155,8	62,4	151,5	171,5	221,5
18,3	0,9	-1,3	157,1	60,9	249,3	349,3	389,3
20,8	0,9	-1,5	154,5	56,0	254,9	304,9	394,9
13,7	1,0	-2,6	156,4	62,2	236,2	336,2	386,2
21,8	0,9	-2,1	157,1	62,4	188,6	228,6	298,6
10,1	1,4	-0,8	155,7	61,4	303,1	383,1	483,1
18,7	1,6	-2,1	156,6	60,8	154,3	184,3	234,3
6,9	1,2	-1,8	162,0	61,4	340,0	430,0	600,0
12,7	0,6	-1,0	156,1	60,5	479,4	599,4	819,4
5,2	1,2	-1,1	154,7	62,2	572,5	682,5	952,5
14,7	1,8	-1,3	155,1	63,5	189,2	219,2	289,2
12,4	1,5	-0,6	157,8	61,2	242,2	282,2	382,2
11,3	0,5	-1,5	155,3	62,3	596,8	696,8	976,8
20,3	1,9	-1,3	157,5	62,3	134,9	154,9	204,9
17,9	4,8	-1,0	155,6	61,8	113,9	133,9	153,9
26,0	1,1	-1,7	155,4	63,3	175,8	205,8	265,8
27,9	2,3	-1,2	156,7	62,9	103,1	123,1	163,1
48,0	1,3	-0,7	155,9	62,8	130,8	140,8	180,8
13,1	2,0	-2,8	157,3	61,9	147,2	167,2	227,2
8,7	1,4	-0,9	154,1	61,2	238,5	418,5	558,5
17,6	2,7	-2,0	156,2	61,3	128,1	148,1	178,1
16,6	0,8	-1,7	156,1	62,0	278,7	338,7	448,7
10,9	7,0	-1,4	157,9	61,5	91,2	111,2	131,2
12,0	0,7	-1,9	156,9	62,6	381,2	461,2	631,2
23,1	1,2	-2,2	155,5	60,1	174,8	194,8	264,8
10,5	3,0	-1,2	158,5	61,7	145,5	175,5	235,5
15,9	1,4	-1,1	157,6	60,3	194,1	234,1	324,1
7,6	2,0	-0,5	158,0	60,9	270,0	340,0	450,0
21,3	1,3	-2,0	156,0	62,5	170,1	190,1	260,1
13,4	0,7	-1,4	159,1	61,0	359,5	439,5	609,5
9,2	1,0	-0,8	154,9	63,2	430,7	500,7	700,7
15,3	0,4	-0,7	156,8	61,6	611,8	681,8	1011,8
14,4	2,5	-1,3	157,2	63,7	137,9	167,9	217,9

APPENDIX B

Details and default values of all the input parameters of the Gringarten and Sauty (1975) analytical formula.

Source :	A Theoretical Study of heat Extraction From Aquifers With Uniform Regional Flow, A. C. Gringarten and J. P. Sauty, 1975.		Cas de Gringarten&Sauty (1975)
Input :			
Name	Symbol	Units	
Water density	rho_w	kg/m3	995
Water calorific capacity	C_w	KJ/kg/K	4,2
Rock density	rho_r	kg/m3	2800
Rock calorific capacity	C_r	KJ/kg/K	0,75
Rate	Q	m3/h	250
Reservoir thickness	h	m	50
Cap rock thermal conductivity	Kr	W/m/K	2,5
Time	t, delta_t	année	30
Porosity	phi	fraction	0,25
Aquifer heat capacity	rho_a*C_a	kJ/m3/K	2619,75
		2*Q*delta_t	1,31E+08
		(Phi+(1-Phi)*(C_r*rho_r)/(C_w*rho_w))	31,34
		2*Kr*rho_r*C_r*delta_t/(C_w*rho_w)^	568,82
Results :			
Well spacing	D	m	1 363